

Investigation of Stress Relaxation Behavior of Carbon-Containing Shape Memory Epoxy Composites

Songjian Yun, Xiaoyan Liang

Department of Mechanics, School of Civil Engineering, Beijing Jiaotong University, Beijing, 100044, China

Correspondence to: X. Liang (E-mail: lxy@bjtu.edu.cn)

ABSTRACT: A series of shape memory epoxy composites reinforced by varied carbon-black (CB) contents were prepared. Stress relaxation tests were performed to characterize the viscoelastic behavior of the specimens at different temperatures. An empirical rheological model was used to simulate the impacts of the temperature and CB content on the viscoelastic behavior of the materials. The results show that the additive of CB particles can significantly improve the stiffness and decrease viscoelastic properties of shape memory epoxy. In addition, parameter analyses in the theoretical simulation present a further understanding about the impact of the additives on the properties of SMPs. © 2012 Wiley Periodicals, Inc. *J. Appl. Polym. Sci.* 129: 1322–1327, 2013

KEYWORDS: thermal properties; viscosity and viscoelasticity; amorphous

Received 20 June 2012; accepted 10 November 2012; published online 3 December 2012

DOI: 10.1002/app.38819

INTRODUCTION

Shape memory polymers (SMPs) are one class of smart materials. They can be fixed into a temporary shape and subsequently recover original shape under the action of an external stimulus. Due to their many unique advantages over shape memory alloys and ceramics, such as low density, high fixture strain, easy processing, wide shape transition temperature, and biocompatibility, the potential applications of SMPs include biomedical engineering,¹ space deployable structures,² microelectromechanical systems,³ etc. Since the first SMP was reported in the 1980s, various SMPs and their composite structures have been introduced, including SMP matrix,^{4–7} particle- or fiber-reinforced SMP composites,^{8–10} SMP foams,¹¹ SMP sandwich structures,^{12,13} etc. Meanwhile, a great number of works have been devoted to the investigation of their thermomechanical behavior and shape memory effect.^{14–24}

Compared with the most common reported thermo-activated SMPs, electro-activated SMPs are more convenient in many engineering applications. The physical mechanism of electro-activated SMPs is heating for the shape recovery means of Joule heating. Recently, various electrically conductive SMP composites have been reported by introducing conductive additives such as carbon particles, carbon fibers or carbon nanotubes into SMP matrix.^{25–27} However, few reports have investigated the impact of inorganic additives on the viscoelastic behavior of SMPs, although it is vital for the materials to work as dynamic sensors and actuators. In this study, epoxy SMP composites with varied carbon-black (CB) contents were synthesized. Stress

relaxation tests were carried out. The effects of CB content and temperature on the viscoelastic behavior of the specimens were analyzed by an empirical rheological model.

SPECIMEN PREPARATION AND EXPERIMENTAL PROCEDURE

The raw materials of epoxy SMP in this study consist of epoxy resin E-51 and curing agent of 4,4'-methylenedianiline (DDM), in which the mass ratio is 100: 15. A commercial CB particle with a mean diameter of 50 μm was used as the additive. The synthesis process of SMP specimens is briefly described as follows: after preheating to 110°C, epoxy resin E-51 is stirred for 20 min at the velocity of 150 rpm by a magnetic-force stirrer. Then, the presetting quantity of the curing agent and CB particles are added and stirred for another 20 min at the velocity of 260 rpm. A homogenous solution is produced. After that, the solution is poured into a mold and dried for 2.5 h at 80°C and subsequently 2 h at 150°C. Finally, four types of specimens are synthesized. Table I lists the formulations of the specimens used in this study, and they are marked as 1# to 4#.

The stress relaxation test was performed by an in-house developed test system and a temperature-controlled environmental chamber. The size of the specimens was 50 × 15 × 3.34 mm³ (length × width × thickness). The temperature was measured with a thermocouple thermometer. To ensure the thermal equilibrium of the specimens, they were equilibrated at least 10 min before each experiment.

Table I. Formulations of the Prepared Shape Memory Epoxy Composites (Mass Ratio)

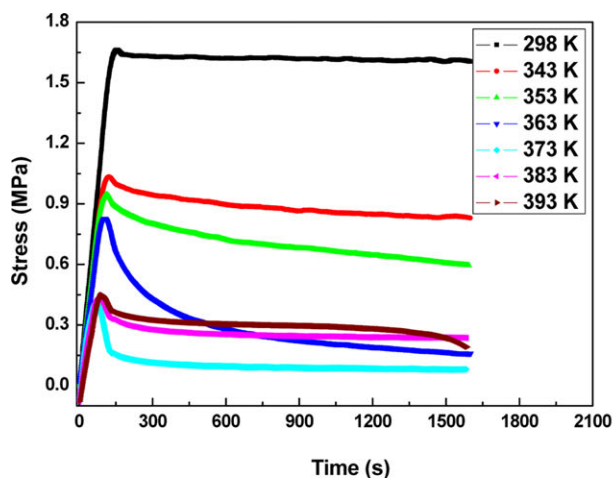
Specimen	1#	2#	3#	4#
E-51	100	100	100	100
DDM	15	15	15	15
CB particles	0	10	15	20

EXPERIMENTAL RESULTS

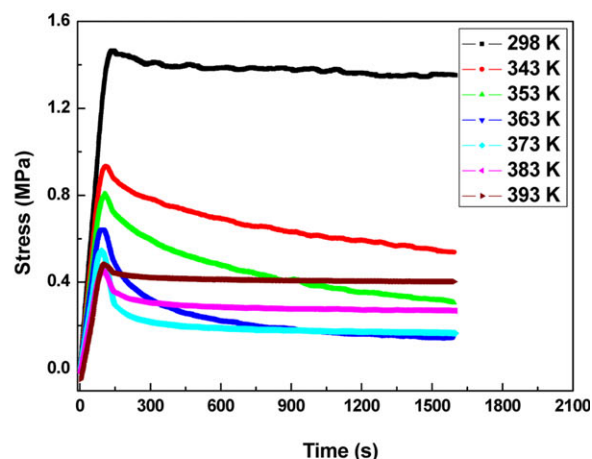
Figure 1 presents the stress relaxation curves of specimens 1# to 4# at different temperatures. The results show that the temperature has a remarkable impact on the stress relaxation behavior of the materials. The stress relaxation is relatively lower at both low and elevated temperatures, but higher at the intermediate temperatures (e.g., 363 K). Moreover, the stress relaxation at the low and elevated temperatures is not symmetrical. It is higher

at elevated temperatures in comparison to that at the low temperatures.

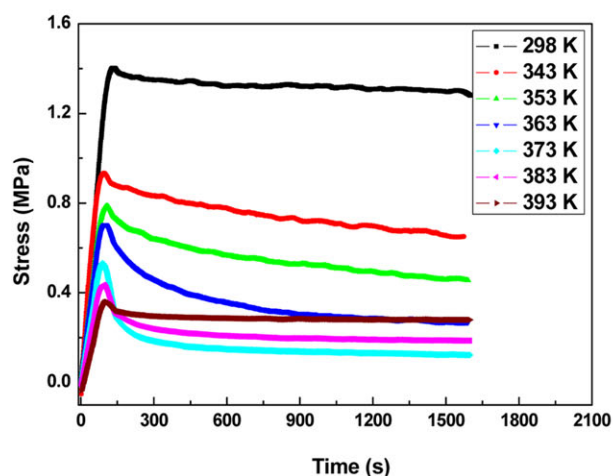
The above experimental results reflect the microstructure features of epoxy SMPs at different temperatures. Epoxy SMPs consist of both crystallites and amorphous chains. The crystallites are elastic-responsive and the amorphous chains undergo a phase change over the range of the test temperatures. When the temperature is well above the glass transition temperature of the material, T_g , the amorphous phase is very soft and the material can have a large deformation via free conformational entropy change, along with some viscous-related deformation mechanisms such as oriented and relative movements of amorphous chains.²⁸ When the temperature is much lower than T_g , the amorphous chains become rigid and the structure is frozen, in which the large-scale conformational changes are not possible and the material behaves as an elastic solid at small strains.¹⁶ The viscoelastic effect in these two states is relatively low. When the test temperature is close to T_g , the viscoelastic effect



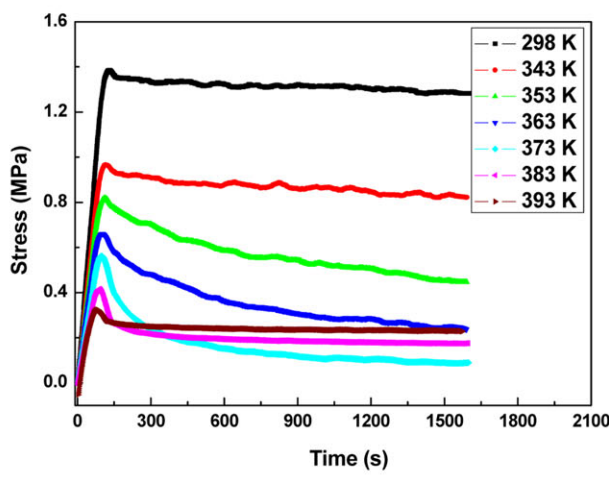
(a) 1#



(b) 2#



(c) 3#



(d) 4#

Figure 1. Typical stress relaxation curves of specimens 1# to 4# at different temperatures. [Color figure can be viewed in the online issue, which is available at wileyonlinelibrary.com.]

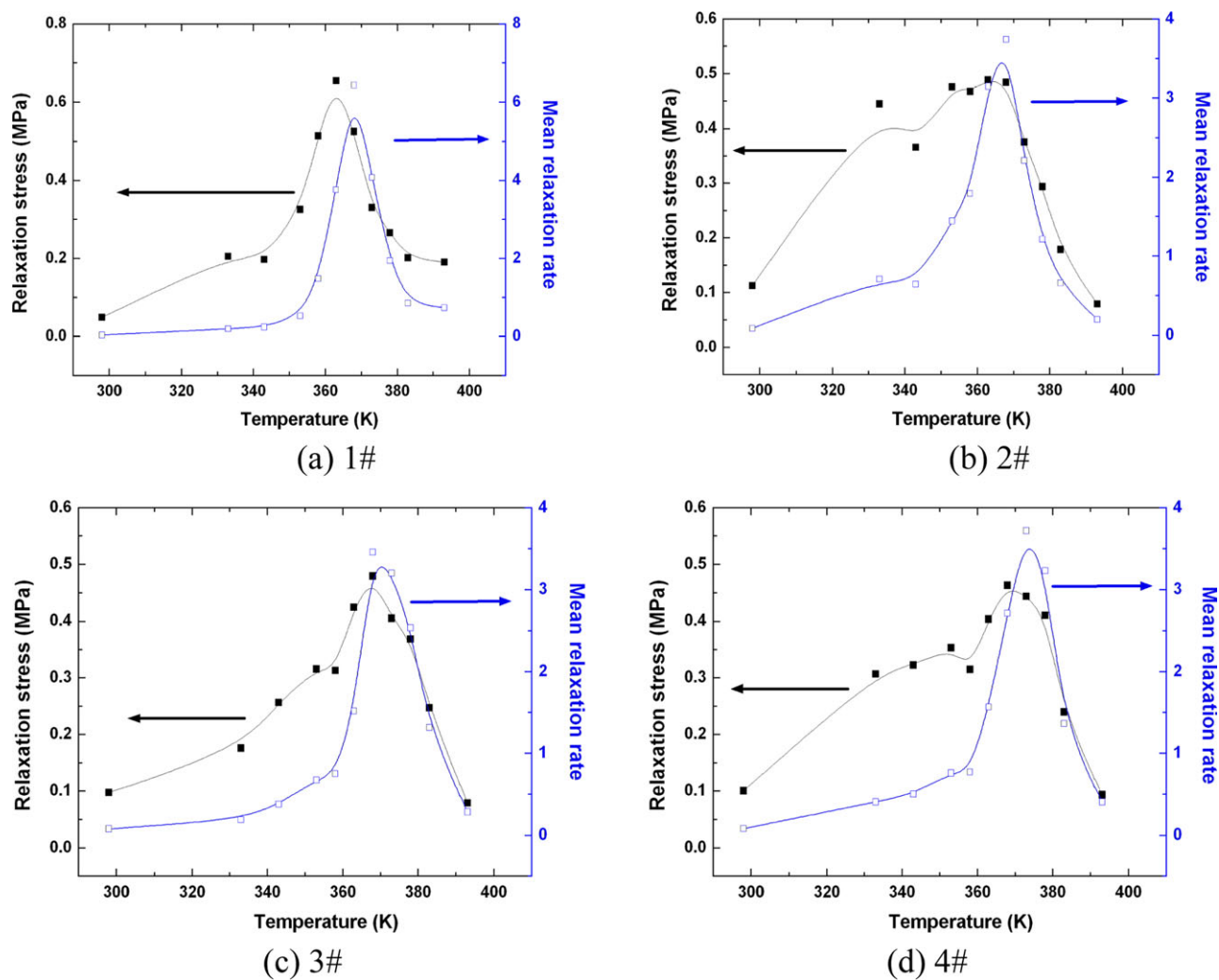


Figure 2. Relaxation stresses and mean relaxation rates of specimens 1# to 4# at different temperatures ($T = 1200$ s). [Color figure can be viewed in the online issue, which is available at wileyonlinelibrary.com.]

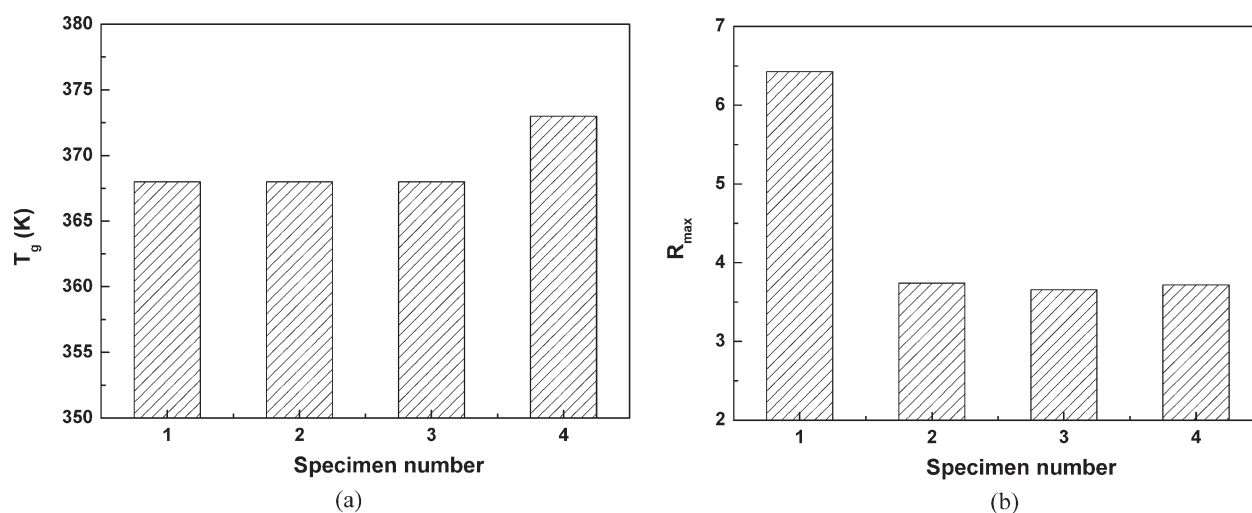


Figure 3. Glass transition temperatures and maximum relaxation ratios in specimens 1# to 4#.

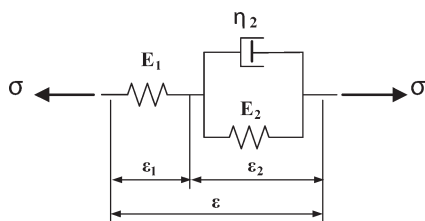


Figure 4. Schematic diagram of linear viscoelastic model. Noted that the crystallites in SMPs are modeled by an elastic spring with the stiffness of E_1 , and the amorphous chains are modeled by a Kelvin model with parameters of E_2 and η_2 .

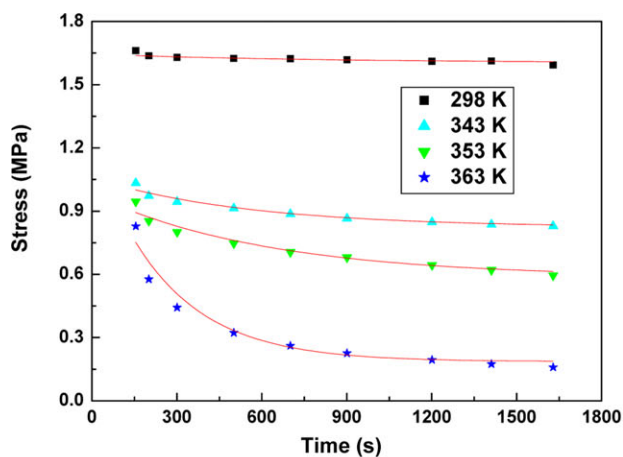
becomes most significant due to the viscous flow of the amorphous phase.

To present a quantitative comparison of the stress relaxation of the materials at different temperatures, two parameters, the relaxation magnitude $\Delta\sigma$ and the relative relaxation ratio R at are introduced and defined as:

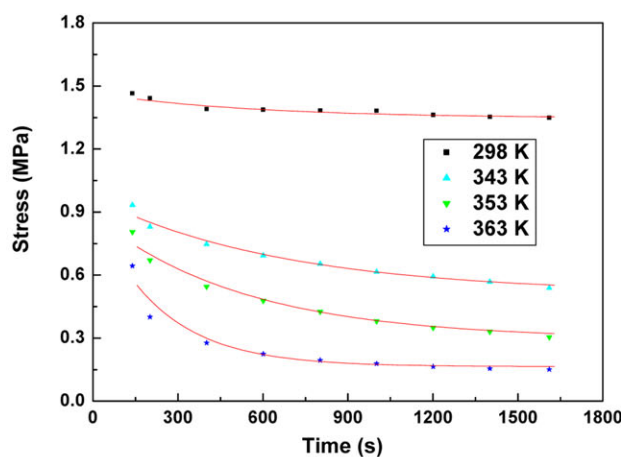
$$\Delta\sigma = \sigma - \sigma_0, \quad R = \Delta\sigma/\sigma_0, \quad (1)$$

where σ_0 and σ denote the initial stress and relaxation stress in the experiment, respectively. Figure 2 shows the experimental results of specimens 1# to 4# at different temperatures. According to Figure 2, $\Delta\sigma$ and R first increase with increasing temperature and then decrease. The T_g of the materials can be determined by the peak value of these curves. Moreover, the results exhibit that the curves of R versus temperatures ($R - T$) are more regular than that of $\Delta\sigma$ versus temperature because the effect of the initial stresses is normalized in the $R - T$ curves.

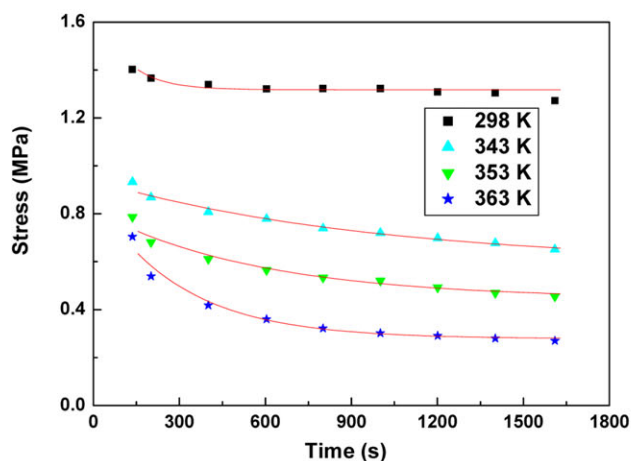
According to Figure 2, Figure 3 presents the glass transition temperature T_g and maximum relaxation ratio R_{max} in specimens 1# to 4#. The results show that the T_g is insensitive at lower CB contents. For example, no difference can be found in T_g for specimens 1#, 2#, and 3#. Only when the CB content reaches 20% in specimen 4#, the T_g value increases from 368 to 373 K. However, the influence of CB content on R_{max} is different.



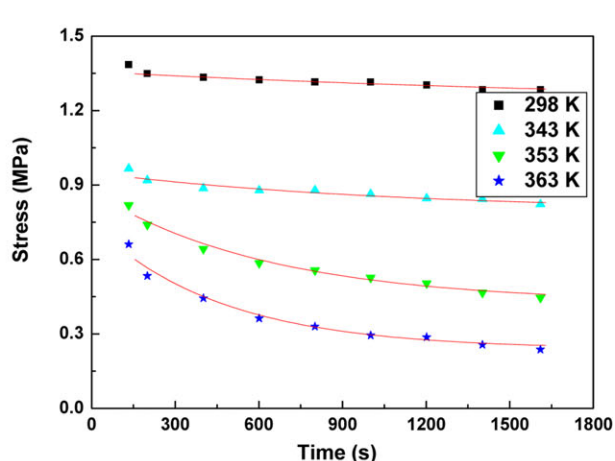
(a) 1#



(b) 2#



(c) 3#



(d) 4#

Figure 5. Experimental and modeling results of the stress versus temperature for specimens 1# to 4#. Note that the experimental and simulating results are represented by solid points and lines, respectively. [Color figure can be viewed in the online issue, which is available at wileyonlinelibrary.com.]

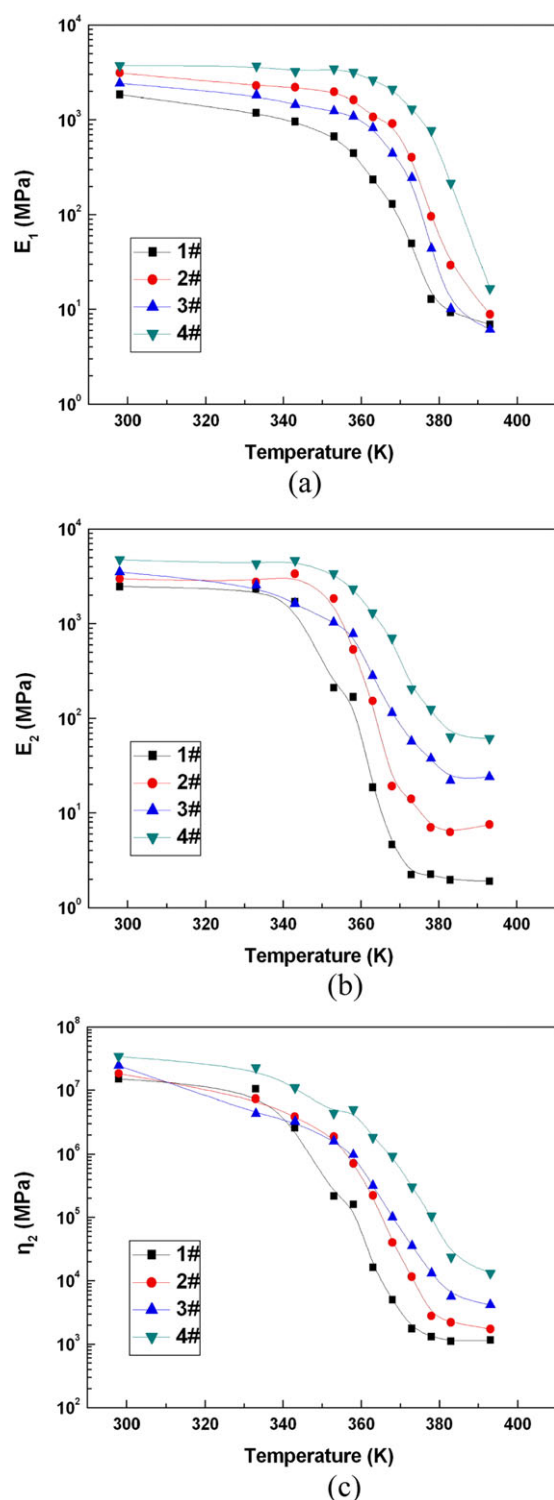


Figure 6. Curves of modeling parameters versus temperatures for specimens 1# to 4#. [Color figure can be viewed in the online issue, which is available at wileyonlinelibrary.com.]

The R_{\max} in pure epoxy SMP is 6.427, whereas it decreases to 3.740 in specimen 2# with 10% CB content, and then no significant difference can be found with further increasing the CB content.

SIMULATION RESULTS AND DISCUSSIONS

Model

In view of the microstructure, the epoxy SMP is a mixture of two phases: crystallites surrounded by amorphous chains. As mentioned above, the crystallites are elastic and the amorphous chains exhibit a viscoelastic response. The shape memory effect is due to the frozen/recovery responses of the amorphous chains as the temperature changes.

To capture the different deformation characteristics of crystallites and amorphous chains, the stress relaxation behaviors of the materials at different temperatures were simulated by a rheological model as illustrated in Figure 4. The viscoelastic response of the amorphous chains was simulated by a Kelvin model, and the elastic response of the crosslinked chains was modeled by a spring. Thus, the stress in the relaxation test can be expressed as

$$\sigma(T, t) = \frac{E_1(T)E_2(T)}{E_1(T) + E_2(T)} \varepsilon_0 + E_1(T)\varepsilon_0 \left(1 - \frac{E_2(T)}{E_1(T) + E_2(T)} \right) e^{-\frac{E_1(T)+E_2(T)}{\eta_2(T)}t} \quad (2)$$

where ε_0 denotes the constant strain in the relaxation test; The Young's moduli, $E_1(T)$ and $E_2(T)$, reflect the instantaneous elastic responses of the crystallites and amorphous chains, respectively; the viscosity, $\eta_2(T)$, reflects the viscous response of the amorphous chains.

Some representative experimental and modeling results are shown in Figure 5. The results show that the modeling curves are in good agreement with the experimental data for specimens 1# to 4#. The dependence of the modeling parameters on temperatures are shown in Figure 6. The results show the influence of CB reinforcement on $E_2(T)$ and $\eta_2(T)$ is higher than that on $E_1(T)$. In addition, the dependence of $E_2(T)$ and $\eta_2(T)$ on CB contents is higher at elevated temperatures than that at lower temperatures. These simulations can be understood in view of the micro-structure of this class of functional materials. CB particles are dispersed in the amorphous phase and naturally affect the viscoelastic properties of the amorphous phase. Moreover, the amorphous chains are very soft at temperatures well above T_g of the material. Thus, the presence of rigid CB particles can significantly improve the stiffness and decrease the viscosity of the material.

CONCLUSIONS

The viscoelastic response has a significant impact on the shape memory effect in SMPs. In this study, the stress relaxation behaviors of epoxy SMPs with varied CB contents were measured at different temperatures. The experimental results were simulated by a rheological model with considering the micro-structure features of epoxy SMPs. The results show that the effects of CB reinforcement on the glass transition temperature and stress relaxation are different. At lower CB contents, the glass transition temperature has no detectable change, but the viscous resistance is greatly increased. At higher CB contents, the glass transition temperature is increased, but the viscous

resistance is lower. Moreover, the theoretical modeling confirms that CB additives can effectively improve the stiffness and viscous resistance of the amorphous phase in the rubbery state.

ACKNOWLEDGMENTS

This work was funded by Natural Science Foundations of China (No 11272044), and the Fundamental Research Funds for the Central Universities (2011JBM074).

REFERENCES

- Lendlein, A.; Langer, R. *Science* **2002**, *296*, 1673.
- Tupper, M.; Gall, K.; Mikulas M. *IEEE* **2001**, *5*, 2541.
- Gall, K.; Kreiner, P.; Turner D.; Hulse M. *J Microelectromech Syst* **2004**, *13*, 472.
- Kim, B. K.; Lee, S. Y. *Polymer* **1996**, *37*, 5781.
- Robin, J.; Martinot, S.; Curtil, A.; Vedrinne, C.; Tronc, F.; Franck, M.; Champsaur, G. J. *Thorac Cardiovasc Surg* **1998**, *115*, 898.
- Alonso, J.; Cuevas, J. M.; Laza, J. M.; Vilas, J. L.; León, L. M. *J Appl Polym Sci* **2010**, *115*, 2440.
- Song, W. B.; Wang, L. Y.; Wang, Z. D. *Mater Sci Eng A* **2011**, *529*, 29.
- Liang, C.; Rogers, C. A.; Malafeew, E. *J Intell Mater Syst Struct* **1997**, *8*, 380.
- Gall, K.; Dunn, M. L.; Liu, Y. P. *Acta Mater* **2002**, *5*, 5115.
- Liu, Y. P.; Gall, K.; Dunn M. L.; Greenberg, A. R. *Mech Mater* **2004**, *36*, 929.
- Prima, D.; Lesniewski, M. A.; Gall, M.; McDowell, D. L.; Sanderson, T.; Campbell, D. *Smart Mater Struct* **2007**, *16*, 2330.
- Wang, Z. D.; Li, Z. F. *Arch Appl Mech* **2011**, *81*, 1667.
- Li, Z. F.; Wang, Z. D. *J Intell Mater Syst Struct* **2011**, *22*, 1605.
- Tobushi, H.; Okumura, K.; Hashimoto, T. *Mech Mater* **2001**, *33*, 545.
- Abrahamson, E. R.; Lake, M. S.; Munshi, N. A.; Gall, K. *J Intell Mater Syst Struct* **2003**, *14*, 623.
- Liu, Y. P.; Gall, K.; Martin, L.; Greenberg, A. R. *Int J Plasticity* **2006**, *22*, 279.
- Kafka, V. *Int J Plasticity* **2008**, *24*, 1533.
- Xiong, Z. Y.; Wang, Z. D.; Li, Z. F.; Chang, R. N. *Mater Sci Eng A* **2008**, *496*, 323.
- Wang, Z. D.; Li, Z. F.; Xiong, Z. Y.; Chang, R. N. *Appl Polym Sci* **2009**, *113*, 651.
- Chen, Y. C.; Lagoudas, D. C. *J Mech Phys Solids* **2008**, *56*, 1752.
- Wang, Z. D.; Li, Z. F.; Wang, Y. S. *J Intell Mater Syst Struct* **2009**, *20*, 1565.
- Srivastava, V.; Chester, S. A.; Anand, L. *J Mech Phys Solids* **2010**, *58*, 1100.
- Zhang, Q.; Yang, Q. S. *Appl Polym Sci* **2012**, *123*, 1502.
- Wang, Z. D.; Li, Z. F.; Wang, L. Y.; Xiong, Z. Y. *J Appl Polym Sci* **2010**, *18*, 1406.
- Cho, J. W.; Kim, J. W.; Jung, Y. C.; Goo, N. S. *Macromol Rapid Commun* **2005**, *26*, 412.
- Paik, I. H.; Goo, N. S.; Jung, Y. C.; Cho, J. W. *Smart Mater Struct* **2006**, *15*, 1476.
- Drubetski, M.; Siegmann, A.; Narkis, M. *J Mater Sci* **2007**, *42*, 1.
- Wang, Z. D.; Zhao, X. X. *Mater Sci Eng A* **2008**, *486*, 517.